ES Materials and Manufacturing
DOI: https://dx.doi.org/10.30919/esmm5f1045

Effect of Different Ag Content on the Structural and Mechanical Properties of Sn15Bi Solder

Yu Ding,[1,*] Fengjiang Wang,[1] Yulin Li[1] and Kaipeng Wang[1]

Abstract

Sn-Bi becomes one of the most potential solders due to its low melting point. In order to improve the function of SnBi solder, Ag is added to it. The microstructure of Sn15Bi solder consisted of primary β-Sn, Sn-Bi solid solution and Bi phase which precipitated along the grain boundary, while the bulk of Bi and many fine Ag_3Sn phase appeared in SnBiAg solder matrix. The solders' melting points were tested by DSC. With the Ag content increased, the melting point decreased. When the content reached 2 wt.%, the melting point was 204.383 ℃, which was about 4% lower than the original solder; The wetting performance was tested by a wetting balancer, when the wetting temperature increased, the wettability got enhanced. Comparing the maximum wetting force and zero-crossing time, when the Ag content was 2 wt.%, the wettability was the best; The analysis of the thickness and growth rate of the IMC showed, the thickness of the IMC increased with the increase of aging temperature and time. However, when the Ag content exceeds 1 wt.%, the growth rate slowed down in later stage of aging process, because Ag_3Sn phase was formed above Cu_6Sn_5 gradually. Ag_3Sn became a barrier, blocking the diffusion of Cu-Sn.

Keywords: Sn-Bi solder; Ag addition; IMC growth; Mechanical properties.
Received date: 25 November 2020; Accepted date: 6 January 2020.
Article type: Research article.

1. Introduction

With the emphasis on environmental protection, People are developing new lead-free solder.[1] Among these lead-free solders, Sn-Ag-Cu solder has been considered the best solder for its excellent performance.[2,3,4] However, the melting point of SAC solder was more than 200℃,too much heat input would cause warping and other deformation phenomena in electronic devices.[5,6] Therefore, Sn-Bi solder got widely used due to its low melting point. But Sn-Bi solder was very brittle, moreover, Sn-based solder would react with Cu substrate to generate Cu-Sn compounds, which were brittle too. Not only that, the compounds would grow up and became more brittle during using.[7,8] Therefore, some alloy elements added into Sn-Bi solder to improve its properties, such as mechanical properties and wettability.[9-13] Chen *et al*.[14] added Ag to Sn-Bi solder to study its electromigration. It was found that Ag_3Sn compounds formed and acted as a barrier to prohibit the migration of Bi from cathode side to anode side. It has been reported that[15], RE was doped into Sn-Bi solder, the eutectic point of the solder alloy decreased slightly, the microhardness and thickness of Cu_6Sn_5 IMC decreased. Some scholars[16] added 0.5 wt.% La into Sn-Bi solder, led the IMC containing RE formed in solder matrix, and enhanced the bonding strength of solder joints during high temperature aging. What's more, the reliability of package can be improved by surface treatments. Electroless nickel immersion gold (ENIG), organic solderability preservative (OSP), Ni-Au, Ni-Pd, and immersion Sn (ImSn), Immersion silver (ImAg)[17] were used to avoid the formation of Cu_6Sn_5. However, in order to promote the reliability, it's necessary to study the wettability and solderability of solder itself, because it affected the bonding of solder and substrate directly.[18,19]

2. Experiment procedure:

2.1 Preparation on solder alloys

Sn15Bi-*x*Ag solder was prepared by pure Sn, Bi and Ag (99.99 wt.%). According to the quality ratio, the metals were smelted with wetting balancer at 380 ℃ covered by a small amount of antioxidant. And the molten solder was stirred repeatedly using a glass rod at least three times at 10 mins intervals. Then kept the melts at 280 ℃ for 12 hours for homogenization. After standing, the liquid metal was poured in a graphite mold

[1] *Provincial Key Laboratory of Advanced Welding Technology, Jiangsu University of Science and Technology, Zhenjiang 212003.China.*
**Email*: JUSTYuDing@163.com (Y. Ding)

and cooled at 25 degrees Celsius. A series of Sn15Bi-*x*Ag solders were prepared respectively (x=0, 0.5, 1 and 2 wt.%).

2.2 Microstructure of alloys and wettability test

To study the microstructures of the solders, scanning electron microscopy (SEM) and energy dispersive X-ray (EDX) were used. For SEM investigation, Sn15Bi-*x*Ag alloys were taken 0.2g, cold mounted with epoxy resin. Then the samples were ground by using different types of sandpaper and polished via diamond slurry, followed by corrosion with 3% dilute HCl. The wettability was tested by wetting balancer (SAT-5100, Rhesca Co. Ltd, Japan). The size of the test copper was 25 mm in length, 1mm in width and 0.215 mm in thickness. Before the test, the copper sheet was cleaned with absolute ethanol and then wiped. During the process, the flux was a water-based VOC-free type (PacIFic 2009MLF, Interflux Electronics NV). The copper sheet was immersed in the solder at a speed of 5mm/s and held for 10s at a depth of 3mm of the liquid solder. And it was separated from the solder at a speed of 5mm/s. Considering the influence of temperature on the wetting performance, three different temperatures (250℃, 260℃ and 270℃) were set in this study.

2.3 Melting point test

The melting points of the solder were tested by a differential thermal analyzer (Diamond DSC, PE, America). The heating rate was 10 °C/min, and the temperature range was from 50 °C to 350 °C, in nitrogen gas with a flow rate of 20.0 ml/min.

2.4 Interfacial structure of joints

The solid state thermal aging tests were implemented via solder joint samples. The joints were prepared by several steps, including solder ball preparation, copper sheet preparation and joint preparation. For the ball preparation, 0.3 g Sn15Bi-*x*Ag solders were weighted and remelted into small balls assisted by solder flux. The copper sheet size was 10 mm × 10 mm × 0.8 mm, polished with sandpaper until there were no scratches on the surface. Then put the solder ball on the copper sheet and soldered at 280 ℃ for 30 seconds in the air. In order to explore the influence of aging temperature and aging time on the compound layers, the joint samples were divided into several parts, which were aged at 120 ℃, 140 ℃ and 160 ℃ for 10 days, 20 days and 30 days respectively. Like the previous bulk solder microstructure observation processes, the joint microstructure and elements observation were also investigated in a same way.

2.5 Shear force of solder joints and tensile properties of solder

A clipper (PTR-1102) was used to measure the shear force of the solder joint before and after solid aging. As the schematic diagram shown in Fig. 1, the shear height was 20 microns, and the speed set as 0.1 mm/s. And the tensile strength of the solder was measured at room temperature.

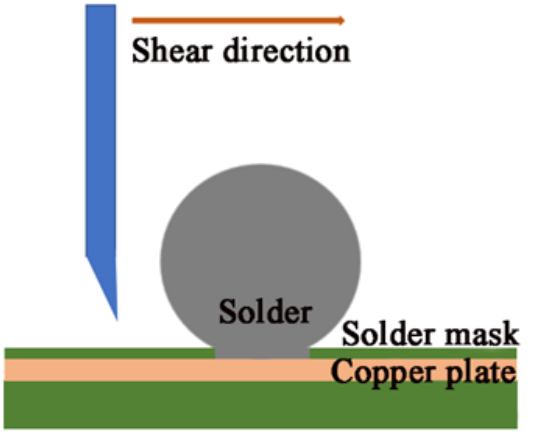

Fig. 1 Schematic diagram of shear test.

3.Results and discussion

3.1 microstructure of solders

Fig. 2 shows the microstructure and EDS results of the solders and Fig. 3 shows the XRD results of the four solders. The microstructures of four solder samples show large difference in beta tin grain size and Bi phase aggregation due to the effect of Ag addition. Without Ag addition, the microstructure of Sn-15Bi contains a large amount of beta tin dendrites (Gray matrix) and eutectic structure (net structure distributed on the matrix). Combined with EDS analysis, it can be seen that the gray phase is β-Sn phase and the white is Bi rich phase. According to the Sn-Bi binary phase diagram, the solid

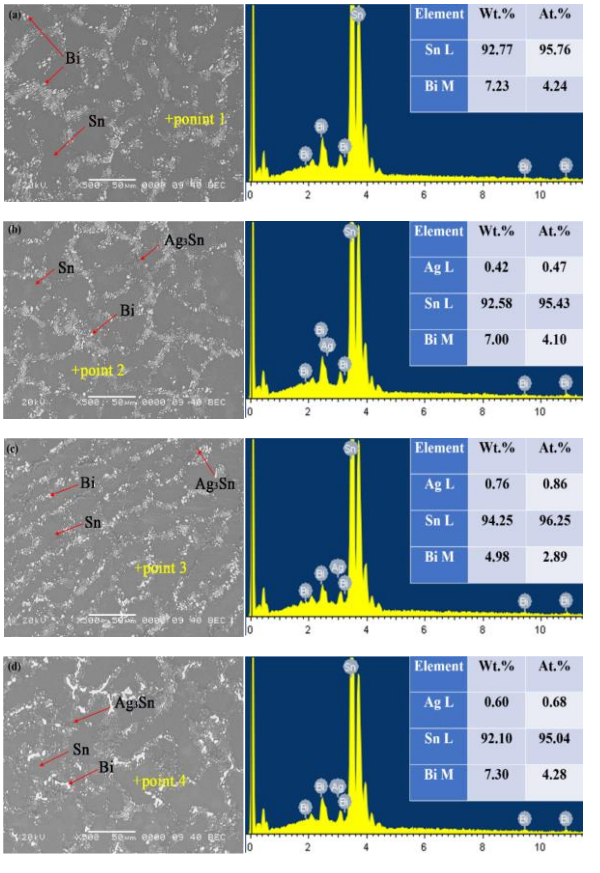

Fig. 2 Microstructure and EDS analysis of Sn15Bi-xAg solder (a) Sn15Bi (b) Sn15Bi-0.5Ag (c) Sn15Bi-1Ag (d) Sn15Bi-2Ag.

solubility of Bi in Sn is only 2 wt.%-3 wt.% at room temperature. During solidification, element Bi will precipitate along the grain boundary of primary beta Sn phase slowly, in the form of small particles. Also, a small amount of Bi may precipitate from beta tin and result in the fine Bi particles formation on Sn-based matrix.[20] As shown in EDS result of Sn-15Bi, there are about 7 wt.% of Bi appeared. As a compound formation element in Sn15Bi-*x*Ag solder alloy, Ag will react with Sn to form Ag_3Sn compound. In the SEM images of Sn15Bi-*x*Ag solder alloy in Fig. 2(b)~(d), small Ag_3Sn phase was found at the grain boundary of β-Sn. And with Ag content increasing from 0.5 to 2, the beta tin dendrite size decreases from 21.6 μm to 16.5 μm gradually, as listed in Table. 1, which indicates that Ag addition can refine the microstructure of Sn-Bi solder.

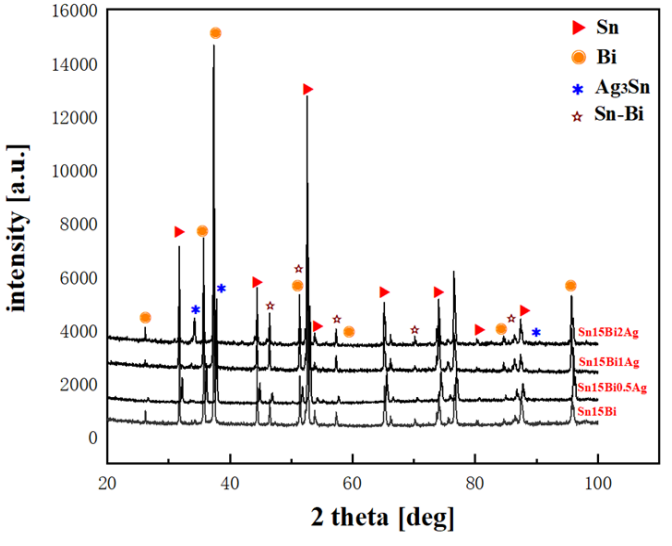

Fig. 3 The XRD patterns of lead-free solders.

Table. 1 Average grain size of the microstructure.

Solder alloy	Beta tin denrite size (μm)
Sn15Bi	21.6
Sn15Bi-0.5Ag	18.9
Sn15Bi-1Ag	18.3
Sn15Bi-2Ag	16.5

3.2 Wettability of solder alloys

Fig. 4 is a schematic diagram of the force in copper sheet during wetting. The copper sheet subjected the surface tension of the liquid solder, before and after immersed in the molten solder. Fmax represents the resultant force on the copper in the vertical direction. The force, F, measured by formula (1):

$$F = \gamma_{LF} \times \cos\theta \times L - \rho V g \quad (1)$$

where F is the resultant force (mN) on the copper sheet, γ_{LF} is the liquid-flux surface tension, θ is the instantaneous contact angle, Lis the liquid meniscus perimeter around the immersed Cu sheet, and ρ is the density of the solder in the molten state, V is the volume of the copper sheet immersed in the liquid solder, and g is the acceleration of gravity. In formula (1), the two terms represent surface tension and buoyancy respectively. After the copper immersed in molten solder, a negative force was first generated on it due to the non-wetting of the solder. When the flux started to work, the molten solder would climb to the surface of the copper sheet. When the surface tension was equal to the buoyancy, the required time was called zero crossing time or wetting time (T0). With surface tension increased, the contact angle θ decreased, and the force acting on the copper plate increased. Finally, the maximum wetting force and the minimum wetting angle were reached within a certain period of time. The zero-crossing time and the maximum force from the wetting curve (usually defined as wetting time and wetting force) were the most important indicators for evaluating wettability. The shorter wetting time or the higher wetting force, the better wettability of the solder alloy.

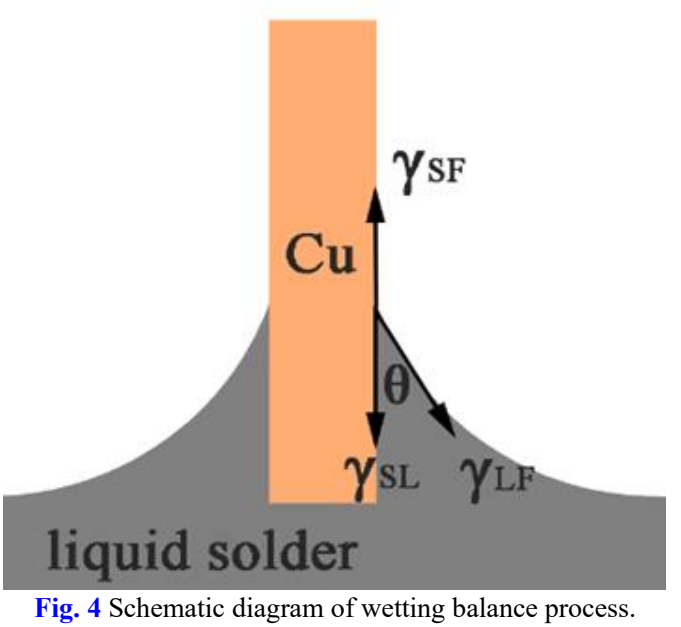

Fig. 4 Schematic diagram of wetting balance process.

Table. 2 T0 and Fmax values of Sn15BixAg (x=0,0.5,1,2) at three temperatures.

Solder	Temperature (°C)	Fmax (mN)	T0(s)
Sn15Bi	250	2.713	0.987
	260	2.73	0.845
	270	2.86	0.826
Sn15Bi0.5Ag	250	2.606	0.886
	260	2.74	0.847
	270	2.72	0.806
Sn15Bi1Ag	250	2.795	0.838
	260	2.716	0.819
	270	2.795	0.814
Sn15Bi2Ag	250	2.783	0.892
	260	3.023	0.79
	270	2.9	0.786

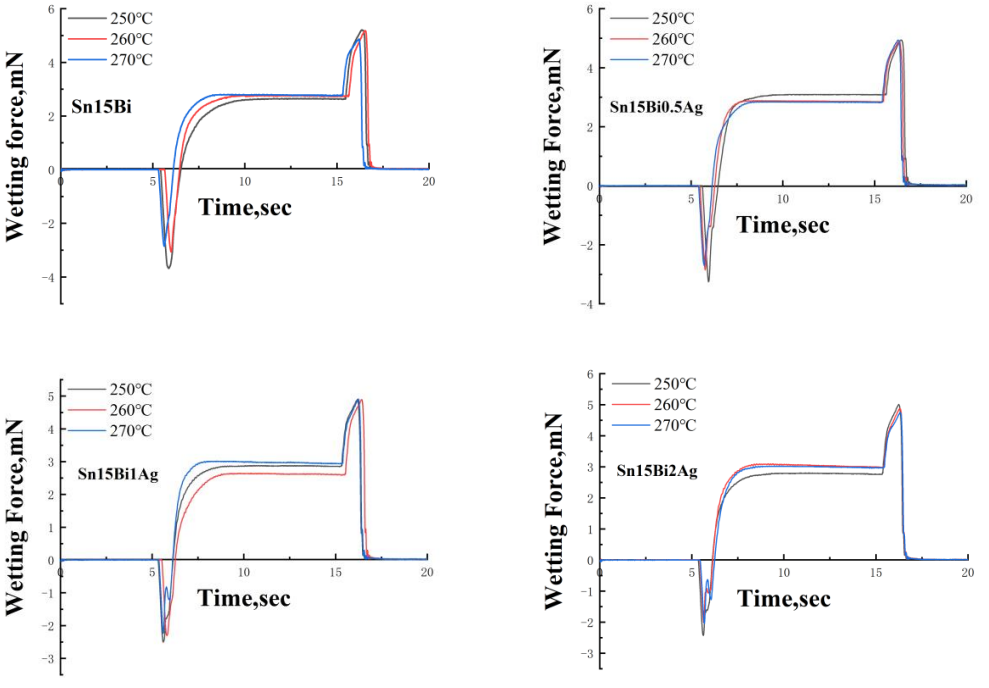

Fig. 5 Wetting curves of Sn-15Bi-xAg (x=0, 0.5, 1and2) solder.

Fig. 5 shows the wetting curves of four different solders at three temperatures. Table. 2 lists the Fmax and T0 values under different conditions. The change of temperature affected the value of T0 intuitively. As the temperature rose, the wetting time decreased. Because under high temperature, the volume of the molten solder would expand, led the distance between molecules increased, so that the force of the bulk molecules on the surface layer molecules decreased, and with the temperature increased, the vapor pressure of the gas phase also increased, which was leading the gas density increased, and made the gas molecules have greater influence on the liquid surface molecules, so the value of surface tension γ became smaller. The relationship between surface tension γ and θ satisfied formula (2)[21]:

$$\cos\theta = (\gamma_{SF} - \gamma_{SL})/\gamma_{LF} \quad (2)$$

Formula 2 shows that the smaller the wetting angle θ, the better the wettability of the solder alloy. Therefore, increasing γ_{SF} or decreasing γ_{SL} and γ_{LF} can reduce the wetting angle θ and improve the wettability. From the physical conception, the surface tension of the solder decreased, the attraction of the atoms in the liquid to the surface atoms weakened, the liquid atoms are more likely to overcome their own gravitational force, and tend to the liquid surface, which would make the spread area larger. So, when the content was 2 wt.%, the solder had the best wettability.

3.3 Melting point of solder

For understanding the relationship between the microstructure and the solidification process, the thermal behavior of Sn15Bi-*x*Ag solders were analyzed using DSC analysis and the results are represented in Fig. 6. As seen, there are two exothermic peaks in the DSC curves of the solders. The low temperature peak appears at about 414k, around the melting point of eutectic Sn-58Bi phase.[22] This peak relates to the eutectic phase transformation from liquid to solid: L→SnBi eutectic. And the second peak shows at 484.8 K, 482.9 K and 478.4 K separately with Ag content increase. According to the ternary phase diagram of Sn-Bi-Ag, it should represent the precipitation of primary beta tin phase: L→L+beta tin primary phase. Additionally, there are not Ag_3Sn phase transformation peak shown in all the DSC curves, which should be ascribed to a higher melting point of Ag_3Sn, about 750 K. Therefore, the Ag_3Sn phase remains solid within the temperature range. Generally, the phase changes during DSC test are listed in Table. 3 with the Sn-15Bi and Sn-58Bi alloy for references.

It's also found that precipitation temperature of primary beta tin is inversely proportional to the content of Ag; the melting point of the solder without Ag was 487.766 K, and when the content of Ag reached 2 wt.%, the melting point decreased to 478.383 K, decreased by about 2%. The melting point of the metal determined by the force between the particles inside the substance. The atoms of the same metal bonded by metal bonds. When foreign atoms enter the crystal, the metal bond destroyed, and the metal arranged in disorder. At this time, the internal energy of the metal increased, and causing the melting point decrease. So, when Ag atoms entered the crystal, the metal bond between Sn destroyed and Ag_3Sn compound formed. The overall process led to a

disordered state in Sn-Bi-Ag alloy. At this time, the internal energy of the solder alloy increased, resulting to a lower phase change temperature.

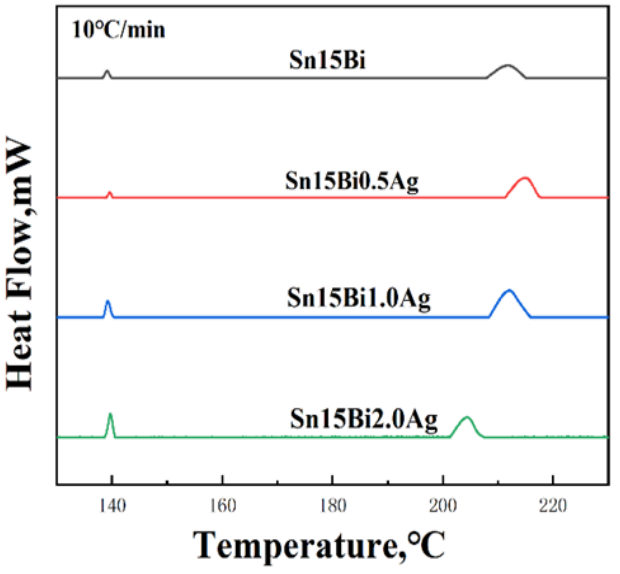

Fig. 6 DSC curves of Sn15Bi-xAg.

Table. 3 The possible Solidification Process.

Solder alloy	Peak 2	Peak 1	Final microstructure
Sn58Bi		L→SnBi eutectic	lamellar structure composed of a metallic phase and a semiconductor phase generally show a complex regular microstructure
Sn15Bi-xAg(x=1,2,3)	L→L+Beta Tin primary phase	L→ Ag_3Sn + (Bi) + (Sn) (peak one) Beta tin→ Particle Bi +Beta tin dentrite (second phase)	Eutectic zone with Ag_3Sn between the phase boundary of Bi rich and Sn rich phase + Beta tin base with Bi particle precipitated

3.4 Sn15Bi-*x*Ag/Cu interfacial aging

During aging, the Sn atoms in the solder and the Cu atoms in the substrate undergo material transfer, Cu_6Sn_5 formed at the interface ($6Cu + 5Sn = Cu_6Sn_5$). In the later stage of aging, a thin layer of Cu_3Sn observed between Cu_6Sn_5 and Cu substrate, because of the reaction of Cu_6Sn_5 and Cu, and also, Cu and Sn($3Cu + Sn = Cu_3Sn$, $9Cu + Cu_6Sn_5 = 5Cu_3Sn$).

Fig. 7 is the secondary electron image of the interface at different times under 140 °C. As the aging time increased, the thickness of the IMC increased. After a little of Ag added, the growth of the compound has been inhibited. This is because the rich Bi layer formed above the IMC, which blocked the material transmission path of Cu and Sn. When the content of silver reached 2 wt.%, Ag_3Sn formed above Cu_6Sn_5, which not only did not inhibit the growth of the compound, but deepened the accumulation of the compound.

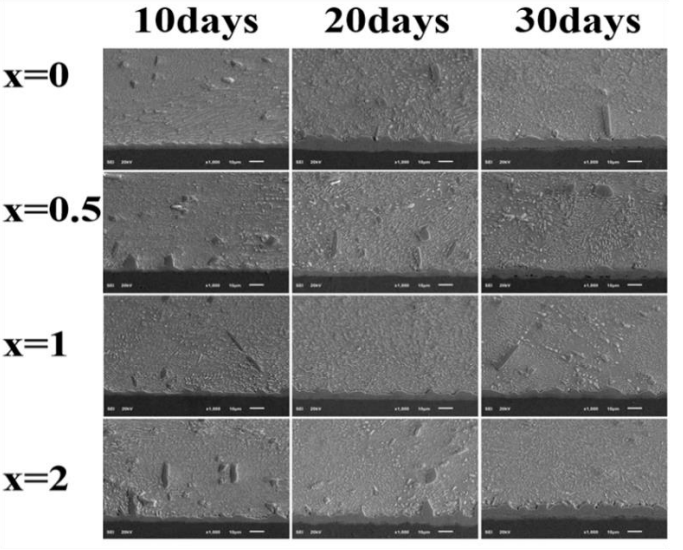

Fig. 7 Interfacial structure of Sn15Bi-xAg solder joints under 140 °C.

3.5 Mechanical properties:

The samples were measured after 30 days aged at 25 °C, the shear fracture occurred in the solder matrix all, which indicated that the mechanical properties of the solder joint were better than those of the solder itself. Wang[23] pointed out, with the increase of aging time, the shear stress of Sn15Bi solder joint increased first and then decreased. That is because in the later stage of aging, the excessive growth of IMC made the solder joint brittle. In this study, the solder joint was aged at room temperature for 30 days, which made the solder joint undergo dynamic recovery process, and the mechanical properties were improved a certain degree of recovery.

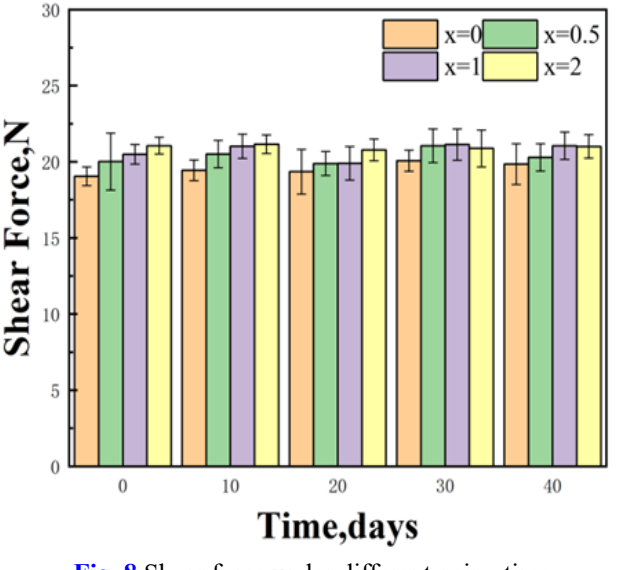

Fig. 8 Shear force under different aging time.

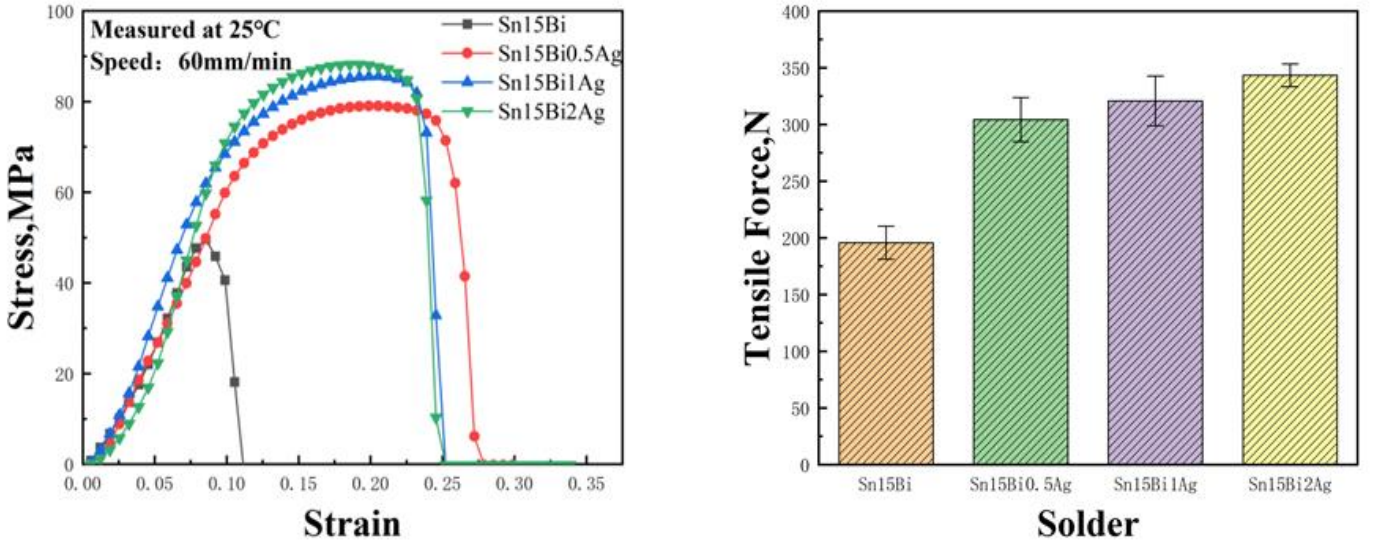

Fig. 9 Stress strain curve and tensile strength.

The cutting data is shown in Fig. 8. The aging time has no obvious effect on the shear force, but the addition of Ag enhanced the mechanical properties of the solder. The addition of Ag promoted the generation of Ag_3Sn in the solder, Ag_3Sn did not react with Sn and Bi, As a result, Ag_3Sn distributed in the solder as a precipitate, which played a precipitation strengthening mechanism.[24] The Bi solubilized in Sn caused lattice distortion, which increased the resistance of dislocation movement and made it difficult to carry out sliding, thus increasing the strength and hardness of solid solution. It played a solid solution strengthening mechanism. The combination of the two metal strengthening mechanisms improved the mechanical properties of the material to a great extent. In Fig. 9, it can be found that when the stress value reached the peak value, it dropped to 0 immediately, so the fracture mode of the three solders were brittle fracture, and with the increase of Ag content, the tensile strength of solder also improved. This is due to the combination of solution strengthening and precipitation strengthening mentioned above.

4. Conclusions:

In this paper, we mainly studied the influence of different Ag content on the properties of Sn15Bi solder, including wettability, interfacial structure growth and melting point. The following achievements can be concluded:

1. The microstructure of Sn-15Bi bulk solder was consisted of primary β-Sn phase and Bi solid solution, and the Bi phase precipitated along the grain boundary. In the microstructure of Sn15Bi-xAg solder, in addition to the phase in Sn-15Bi, there was also fine Ag_3Sn phase.
2. The thickness of the interface compound increased with the increase of aging temperature and aging time. When Ag content was more than 1wt.%, the formation of Ag_3Sn above Cu_6Sn_5 inhibited the growth of the compound.
3. When the Ag content was 2wt.%, the wettability of the solder was the best, this performance is good for the spreading of solder on the substrate.
4. The melting point of the solder decreased when the Ag content increased, this can reduce the heat input during soldering, and improve the reliability of electronic packaging.
5. The addition of Ag caused Ag_3Sn formed in the solder. The precipitation strengthening mechanism brought by Ag_3Sn, combined with the solid solution strengthening mechanism brought by Bi, which greatly improved the mechanical properties of the solder.

Acknowledgement

The authors would like to acknowledge the support provided by the National Natural Science Foundation of China (Grant No. 51875269).

Conflict of interest

The authors declare that they have no conflict of interest.

Reference:

[1] H. R. Kotadia, P. D. Howes, S H Mannan, *Microelectron. Reliab.*, 2014, **54**, 1253-1273. doi: 10.1016/j.microrel.2014.02.025.

[2] L. Zhang, J. Han, Y-h. Guo, L. Sun, 2014, *J. Mater. Sci. Mater. Electron.*, 2014, **25**, 4489-4494. doi: 10.1007/s10854-014-2192-8.

[3] Mostafa Shalaby R, M. Kamal Ali EAM, M. S. Gumaan, *Mater. Sci. Eng. A*, 2017, **690**, 446-452, doi: 10.1016/j.msea.2017.03.022.

[4] M. S. Gumaan, *J. Mater. Sci. Mater. Electron.*, 2020, **31** , 10731-10737, doi: 10.1007/s10854-020-03623-0.

[5] L. Zhang, J-g. Han, Y-h. Guo, C-w. He, *Mater. Sci. Eng. A*, 2014, **597**, 219-224, doi: 10.1016/j.msea.2013.12.098.

[6] R. S. Sidhu, R. Aspandiar, S. Vndervoort, D. Amir, G. Murtagian, *JOM*, 2011, **63**, 47-51. doi: 10.1007/s11837-011-0174-3.
[7] A. K. Gain, T. Fouzder, Y. C. Chan, W.K.C. Yung, *J. Alloy. Compd.*, 2011, **509**, 3319-3325. doi: 10.1016/j.jallcom.2010.12.048.
[8] C. C.Chang, Y.W. Lin, Y. W. Wang, C. R. Kao, *J. Alloy. Compd.*, 2010, **492**, 99-104, doi: 10.1016/j.jallcom.2009.11.088.
[9] F. Wang, L. Zhou, X. Wang, P. He, *J. Alloy. Compd.*, 2016, **688**, 639-648, doi: 10.1016/j.jallcom.2016.07.084.
[10] B. L. Silva, A. Garcia, J. E. Spinelli, *Mater. Charact.*, 2016, **114**, 30-42. doi: 10.1016/j.matchar.2016.02.002.
[11] R. M. Shalaby, *Mater. Sci. Eng. A*, 2013, **560**, 86-95, doi: 10.1016/j.msea.2012.09.038.
[12] F. Wang, Y. Huang, C. Du, *Mater. Sci. Eng. A*, 2016, **668**, 224-233, doi: 10.1016/j.msea.2016.05.072.
[13] G. Ren, I. J. Wilding, M. N. Collins, *Mater. Sci. Eng. A*, 2016, **665**, 251-260, doi: 10.1016/j.jallcom.2016.01.006.
[14] C-m Chen, C-c Huang, *J. Alloy. Compd.*, 2008, **461**, 235-241, doi: 10.1016/j.jallcom.2007.07.059.
[15] C. Wu, J. Shen, C. Peng, *J. Mater. Sci. Mater. Electron.*, 2011, **23**, 14-21, doi: 10.1007/s10854-011-0383-0.
[16] Y-Y Shiue, T-H Chuang, *J. Alloy. Compd.*, 2010, **491**, 610-617, doi: 10.1016/j.jallcom.2009.11.017.
[17] M. Sona , K.N. Prabhu, *J. Mater. Sci. Mater. Electron.*, 2014, **25**, 1446-1455, doi: 10.1007/s10854-014-1749-x.
[18] Q. V. Bui,S. B. Jung, *J. Mater. Sci. Mater. Electron.*, 2013, **25**, 423-430, doi: 10.1007/s10854-013-1605-4.
[19] B.L. Silva, N. Cheung, A. Garcia, J. E. Spinelli, *Mater. Lett.*, 2013, **142**, 163-167, doi: 10.1016/j.matlet.2014.11.088.
[20] F. Q. Hu, Q. K. Zhang, J. J. Jiang, Z. L. Song, *Mater. Lett.*, 2017, **214**, 142-145, doi: 10.1016/j.matlet.2017.11.127.
[21] K. M. Martorano, M. A. Martorano, S. D. Brandi, *J. Mater. Process. Tech.*, 2009, **209**, 3089-3095, doi: 10.1016/j.jmatprotec.2008.07.015.
[22] S. Zhou, S. He, H. Nishikawa, *J. Nanosci. Nanotechno.*, 2020, **20**, 106-112, doi: 10.1166/jnn.2020.17268.
[23] F. Wang, Y. Ding, L. Liu, Y. Huang, M. Wu, *J. Electro. Mater.*, 2019, **48**, 6835-6848, doi: 10.1007/s11664-019-07473-3.
[24] M. S. Gumaan, R. M. Shalaby, E. A. M. Ali, M. Kamal, *J. Mater. Sci. Mater. Electron.*, 2018, **29**, 8886-8894, doi: 10.1007/s10854-018-8906-6.